Cavity Characteristics' dependence on Cavity Length

Webster, Kyle (68017623)

February 28th, 2024

Lab name: Cavity Optics
Lab station: PHAS-OPTICS7
Lab section: L2B
Assigned TA: Reza Rezae
Lab #: 1st
Note to teaching team: Missed 2 sessions due to transit strike and sickness.

Abstract

Optical cavities have many applications and as such are important to understand when learning optics. To that end, the behaviour of parameters that characterize the properties of optical cavities with respect to the cavity length was investigated through seven experiments. First, the components that form the resonant cavity were investigated theoretically and practically; the influence of mirror reflectivity and beam parameters on the cavity was shown theoretically and the values were found experimentally. Before attempting to observe the resonant properties of the cavity, the ideal positioning of the setup was found theoretically. Then, scanning the cavity with a piezoelectic element, cavity modes were observed and analyzed. Interestingly, the resonant modes observed depended on the length of the cavity, as did the computed spectral linewidth of the transmission. Ince-Gaussian 31 and 42 modes were observed in a 23.6cm cavity, and the spectral linewidth decreased with increasing cavity length, agreeing with the expected theoretical result.

RESEARCH NOTE

It was found that the order of cavity modes present is proportional to the cavity length. This was determined through an investigation into the behaviour of the characteristic parameters of resonant cavities with respect to the cavity length. To probe the present cavity modes, a piezoelectric element was used to vary the cavity length on the scale of the light in the cavity.

Scanning the cavity length and recording a fraction of the transmitted power with a camera allowed for the transition between cavity modes to be analyzed. Repeating this at multiple cavity lengths revealed that longer cavities produced higher order and less circularly symmetric modes than at shorter cavity lengths. This is due to the fact that the radius of the beam at the spherical mirror being moved becomes larger, as $R(z) = z + z_0^2/z$, allowing for wider distributions of the beam, as happens at higher modes, to be present in the cavity.

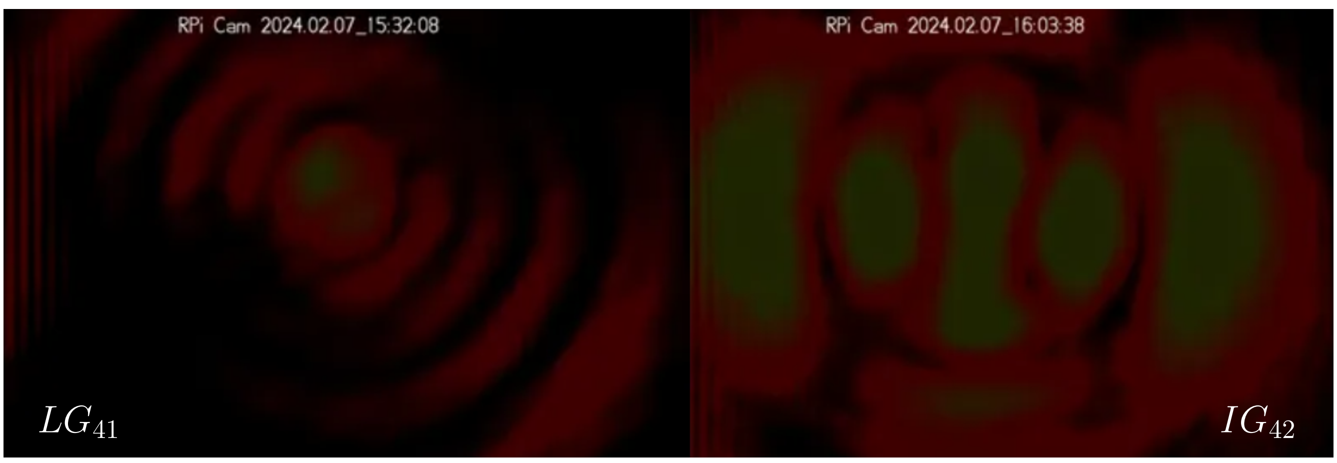

Figure 1: The highest observed TEM$_{lm}$ modes in a short (7.9cm) cavity, left image, and a long (23.6cm) cavity, right image. This result demonstrates that longer cavity lengths lead to higher order cavity modes being observable. Note that low order modes were more intense for both cavity lengths. LG refers to Laguerre-Gaussian modes, and IG refers to Ince-Gaussian modes.

EXPERIMENTS

All experiments used a 20mW HeNe laser, $\lambda = 633$nm, with optical elements as described in each section. A diagram of the setup can be found in Figure 2 for reference.

1 Mirror Reflectivity

Mirrors M1 and M2 characterize the optical cavity by their reflectivity and transmission, and radius of curvature.

(A) The reflectivity and transmission of both cavity mirrors were measured using a power meter. The determined values were $R_{M1} = 0.8475$, $T_{M1} = 0.0123$, $R_{M2} = 0.9836$, $T_{M2} = 0.0037$ each with uncertainty ± 0.0005. Note the reflectivity and transmission do not add to one as some power is lost to scattering and that the measurements for reflectivity and transmission were likely made at large enough distances for the beam to be larger than the power meter sensor. Ideally, these coefficients should at to unity.

(B) Using formula 10.1-14 from [Saleh and Teich(2019)], $\mathcal{F} = \frac{\pi\sqrt{r}}{1-r}$ with r the reduction of the amplitude of a wave over once cycle of the cavity, the finesse we expect is 34.5 ± 0.3 as we assume negligible loss between the mirrors and find r by taking the square root of the product of the reflectivity of each mirror. The square root is essential as the reflectivity is in terms of the power, which goes by the square of the wave amplitude.

(C) For a cavity with length $L = 15$ cm, using formula 10.1-6 from [Saleh and Teich(2019)], $\text{FSR} = \frac{c}{2L}$, we expect a free spectral range of ≈ 1000 MHz. Calculating the linewidth from this FSR and the expected finesse using formula 10.1-19 from [Saleh and Teich(2019)], $\delta\nu_{\text{FWHM}} \approx \frac{\text{FSR}}{\mathcal{F}}$, we might expect to find a linewidth of approximately 29 MHz.

(D) As the reflectivity of the mirrors decrease, the finesse of the cavity decreases as decreases. For the characteristics of the cavity, the linewidth of the cavity would increase as it is inversely proportional to finesse, whereas the free spectral range would remain the same as it is independent of the finesse.

2 Laser Beam Radius

To characterize the beam input into the cavity, the beam waist parameter was determined using the "knife edge" method. M1 was replaced with a knife edge element and M2 was removed so that the unblocked laser intensity may be measured. The position of the knife edge was adjusted by running a MATLAB script that controlled the translation stage.

(A) Referencing the derivation of the expression for the beam waist parameter using the inverse complimentary error function given in section 2.3.2 of the Cavity Optics lab manual [Milner(2023)], the beam waist can be computed by $w = 1.19(x_{20\%} - x_{80\%})$, where $x_{20\%}$ is the amount of the beam covered such that the transmitted intensity is 20% of the maximum and likewise for $x_{80\%}$. This gave a beam waist of 0.27 ± 0.01 mm.

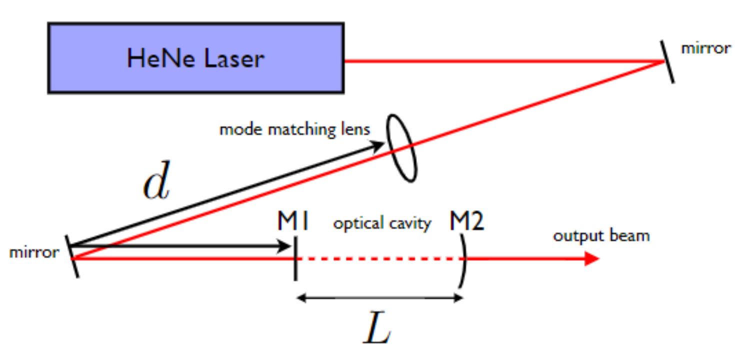

Figure 2: The general experimental setup. A flat mirror M1 and spherical mirror M2 with a radius of curvature of 30cm form the optical cavity. M2 is mounted on a piezo to scan the cavity length on the scale of the laser wavelength, and M1 is mounted on a translation stage. The mode matching lens has focal length 50cm.

(B) By shifting and scaling the data to a normalized range, the full set of data was used to fit the theoretical intensity curve given by

$$\bar{I}(x_k) = \frac{1}{2}\text{erfc}\left(\sqrt{2}\frac{x_k}{w}\right), \qquad \text{erfc}(z) = 1 - \frac{2}{\sqrt{\pi}}\int_0^z e^{-t^2}dt$$

to the data with a single parameter w. This gave a beam waist of 0.283 ± 0.003 mm.

(C) Since the output of the HeNe laser has a beam diameter of 1.2mm and has a very large Rayleigh length, passing it through the mode matching lens with focal length 50cm, the new beam waist parameter is given by equation 3.2-15 from [Saleh and Teich(2019)], $w_0' \approx \frac{\lambda}{\pi w_0} f$. Therefore, we expect a beam waist of approximately 0.085mm.

(D) Clearly, our calculated and expected beam waist values are different. It is likely because we did not measure the beam waist directly at the focus of the transmitted beam.

3 Mode Matching

To measure strong cavity modes, the theoretically ideal conditions should be identified and attempted to be recreated. This experiment determines what those conditions are and does not use the experimental setup.

(A) See Figure 3 for the beam shape and phase fronts of the cavity mode.

(B) In order to best mode match into the cavity, the phase fronts of the incoming beam should have an infinite radius of curvature at M1. Therefore, focusing the incoming beam at M1 would be ideal.

(C) Again, to best mode match into the cavity, the radius of curvature of the beam should match the radius of curvature of M2. The radius of curvature of the beam at M2, $R_{M2} = R(L)$, is given by $R_{M2} = L + z_0^2/L$ from putting $z = L$ into equation 3.1-9 of [Saleh and Teich(2019)]. Recalling that the Rayleigh length and beam waist parameter are related by equation 3.1-11 of [Saleh and Teich(2019)], $w_0 = \sqrt{\lambda z_0/\pi}$, the ideal beam waist at M1 to match curvatures at M2 is found by replacing z_0 with w_0 by 3.1-11 and solving for w_0. We get

$$w_0 = \left(\frac{(R_{M2} - L)\lambda^2 L}{\pi^2}\right)^{1/4}$$

We used cavity lengths between 1 and 24 cm. This gives ideal beam waists ranging from 0.1 to 0.16 mm.

(D) Ideally the choice of focal length and distance from M1 would focus the incoming beam to have the ideal beam waist at the focus of the beam. Since the beam incident on the mode matching lens is collimated, we can use equations 3.2-15 and 3.2-16, $z' \approx f$, in [Saleh and Teich(2019)]. Since we want the phase fronts to have infinite radius of curvature at M1, the ideal mode matching lens is placed a distance equal to it's focal length from M1. Rearranging 3.2-15 for the focal length, $f = \pi w_0' w_0/\lambda$, we see the ideal focal length would be 62.0cm for the 1cm cavity or 92.6cm for the 24cm cavity.

(E) If only M1 is placed in the path of the beam, the transmitted light is slightly reduced in intensity due to some of the incoming beam being reflected instead of transmitted. The phase fronts of the transmitted light still appear as they do in Figure 3.

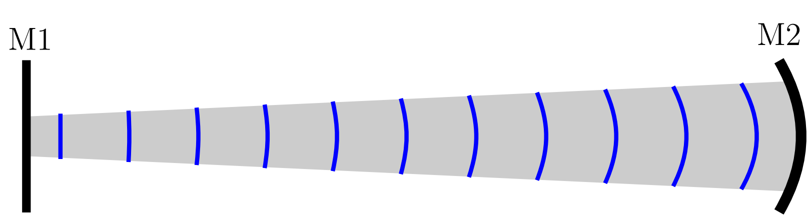

Figure 3: Diagram showing the beam shape (shaded grey area) and phase fronts (blue curves) of the resonant cavity mode. Note that the phase fronts match the shape of M1 and M2 and that the beam radius grows with the cavity length.

(F) Once both mirrors are in place and if the cavity is properly aligned, the intensity of the transmitted light is should be slightly reduced compared to the input beam. However, if the cavity is poorly aligned, the intensity of the transmitted light should be greatly reduced as light reflected off of M2 is not reflected off of M1 back toward it, which would give the light a 'second chance' at being transmitted through the cavity.

4 Cavity Scanning

This experiment uses the exact experimental setup as described in Figure 2. The output beam is split so that a fraction of its power is sent to a Raspberry Pi CCD camera and the remainder to a sensor connected to an oscilloscope.

For a cavity to resonate with a single wavelength λ, its length must be a multiple of $\lambda/2$. To demonstrate this result, the cavity's length is varied on the scale of λ using a piezoelectric element. By scanning the length of the cavity with the piezo, the transmission properties of the cavity as a function of its length are investigated.

(A) Before beginning the piezo scan, the transmitted light as seen on the Raspberry Pi camera appears to mode match with random high-order circular modes. However, when the piezo scan is started, the image appears to be a constant radially symmetric distribution. When the frequency of the scanning is reduced the progression of the intensity through different modes is apparent, there are some modes that are much more intense than others, corresponding to the cavity modes.

(B) From the piezo spec sheet, the piezo moves a distance of 6.1×10^{-8} m per volt applied. Hence, a voltage of 5.1885V shifts the M2 mirror by $\lambda/2$.

(C) The scanning results can be seen in Figure 4.

5 Cavity Modes

The remaining experiments use the same setup described in experiment 4.

When scanning the cavity with the piezo at a lower frequency of 0.05Hz, the transition between transmitted modes is observed on the Raspberry Pi cameras. This experiment identifies the modes and the behaviour of them by analyzing a video of the transitions at two cavity lengths.

(A) The Laguerre-Gaussian modes that were identifiable are shown in Figure 5 for both cavity lengths. The largest Laguerre-Gaussian modes identified were 40 and 41 for the short cavity and 34 for the long cavity. For the long cavity, 31 and 42 even Ince-Gaussian beam modes were observed.

(B) The highest observed mode was a Laguerre-Gaussian 43.

(C) The peaks in brightness are periodic over the scan of the cavity as the transmission peaks when the cavity length is a multiple of $\lambda/2$. Since the piezo scan changes the length of the cavity by more than half a wavelength the peaks repeat during a scan. The lower cavity modes tended to have a higher intensity at the camera.

(D) For different cavity lengths, the size of the beam at M2 is also different. For a longer cavity, the beam width at M2 will be larger. This means that the cavity modes that satisfy the boundary conditions for resonance will change with the length of the cavity.

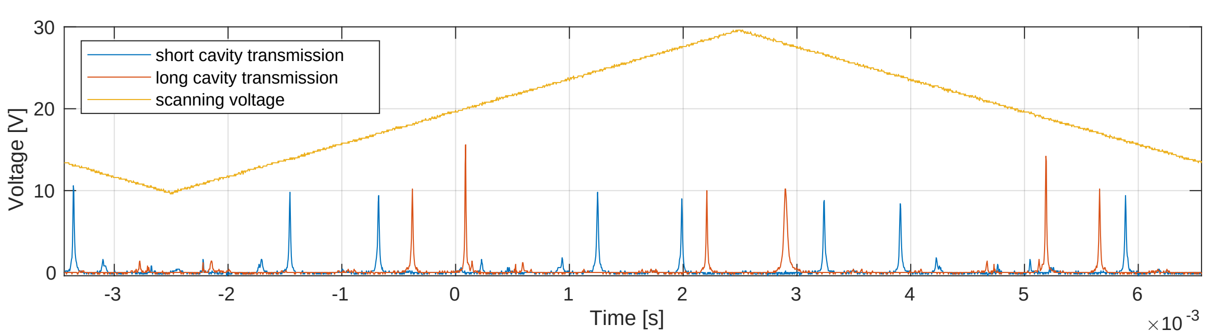

Figure 4: Oscilloscope readings when scanning the cavity at a short, 7.9 ± 0.1 cm, and a long 23.6 ± 0.1 cm length. A triangle wave with peak-to-peak amplitude 2V and frequency of 100Hz was input into high voltage power supply with a gain 10 which powers the piezo. Note that the spikes in transmission correspond to the cavity modes.

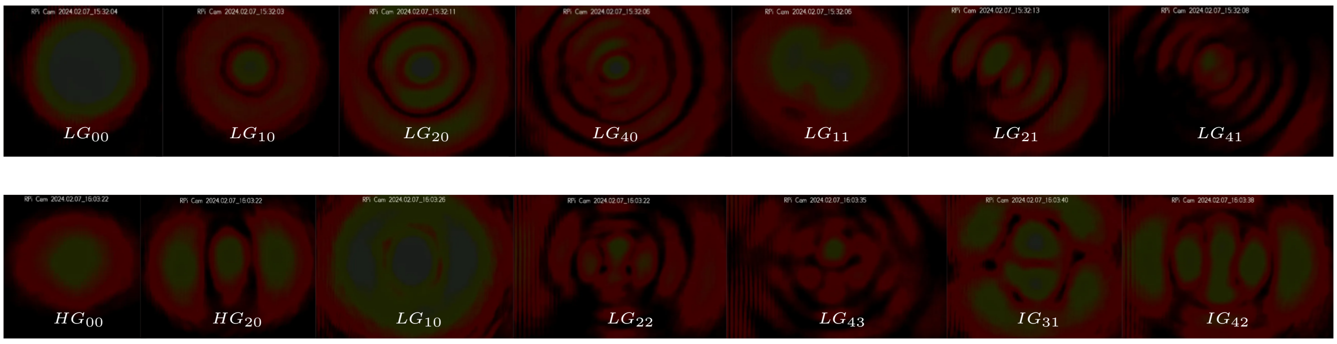

Figure 5: Frames from videos of the scans of the short and long cavity. The top row is for the 7.9 cm cavity and the bottom is for the 23.6 cm cavity. HG refers to Hermite-Gaussian, LG to Laguerre-Gaussian, and IG to even Ince-Gaussian modes. The long cavity has more higher order modes compared to the short cavity.

6 Cavity Finesse

A cavity can be characterized by its free spectral range and the width of its transmission peaks. In this experiment, those parameters are measured and the finesse will be computed.

(A) Measuring the time between peaks and the time to traverse a single peak, as seen in Figure 6, the following table was produced:

Cavity Length [cm]	$t_{\text{period}} \cdot 10^{-3}$ [s]	$t_{\text{FWHM}} \cdot 10^{-6}$ [s]
1	2.604	14
2	2.532	18
5	2.752	14
12	2.624	18
20	2.616	18

Looking for trends in the table, t_{period} and t_{FWHM} remain reasonably constant. This makes sense as the expected finesse was independent of the cavity length.

(B) Considering equation 10.1-19, $\delta\nu \approx \nu_F/\mathcal{F}$, from [Saleh and Teich(2019)], we see the finesse is the ratio between the frequency spacing ν_F and the spectral width $\delta\nu$. From the shape of our traces, we infer that the finesse is the ratio of t_{period} to t_{FWHM}. That is,

$$\mathcal{F} \approx \frac{t_{\text{period}}}{t_{\text{FWHM}}}$$

A plot of this approximate finesse as a function of the cavity length can be found in Figure 7. Recall from the first experiment we expected a finesse of approximately 34.5. This value is considerably lower than the measured finesse and is likely due to a poor measurement of the reflectivity and transmission of the M1 mirror. Although the results do not agree precisely, the trend of the measured finesse to not change with the cavity length is what was expected. This is because the finesse is a measure of how lossy a resonator is and we approximated zero loss when propagating through air, meaning the length of the resonator does not impact its lossyness.

(C) See Figure 7 for the plot of linewidth as a function of the cavity length. As the plot is logarithmically scaled in the linewidth, the agreement appears to be better than the finesse, although it is still not very good. The shape of the computed linewidth *is* what was expected though.

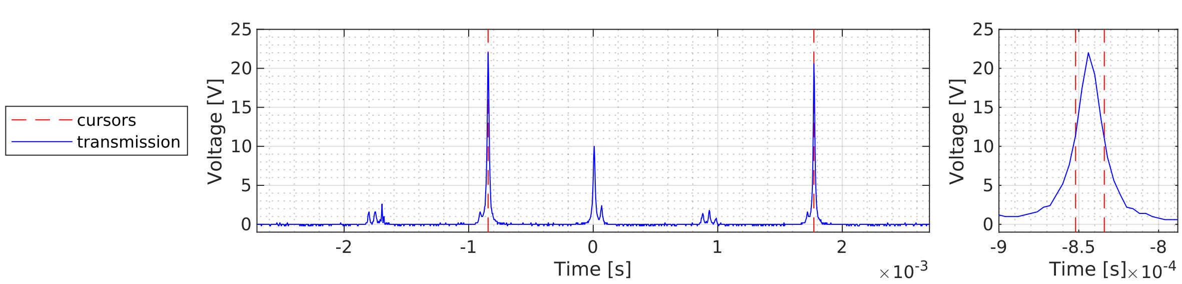

Figure 6: Oscilloscope traces for the 20cm cavity. The left plot shows the measurement of t_{period} and the right plot likewise for t_{FWHM}. The periodicity of the cavity modes over a piezo scan is evident in the left plot.

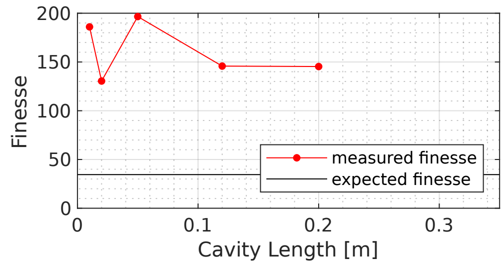

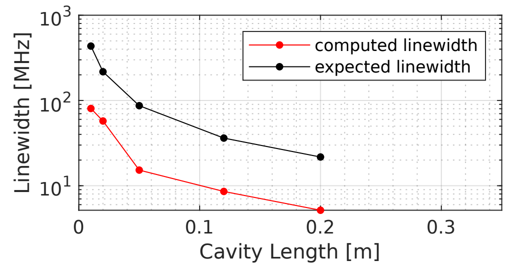

Figure 7: Measured vs expected finesse (left) and linewidth (right). Note the reasonable agreement between the measured and expected values for the 5cm and 12cm long cavities. Also note the cavity length dependence of the finesse that was not predicted by the expected finesse.

(D) From the right plot in Figure 7 it is clear that the linewidth of a cavity/optical resonator decreases with increasing cavity length. It is likely that to make the spectral linewidth of the HeNe laser as small as possible, the resonator inside is made as long as possible.

7 Cavity Stability

This experiment shows that there is a set of cavity lengths that form a stable resonator.

(A) Referencing Appendix D of [Milner(2023)] on resonator theory, the general stability condition given by equation D.1 becomes $0 \leq 1 - \frac{L}{R_{M2}} \leq 1$ for our system which when rearranged for L gives us the range of lengths the cavity may take and remain stable. That is,

$$0 \leq L \leq R_{M2} = 0.30 \ [m]$$

must hold for the cavity to be stable.

(B) When setting the cavity length slightly below R_{M2}, transmission peaks as seen at much shorter lengths are very apparent. As the cavity length approaches the unstable region, the peaks maintain the same spacing, but become very small amplitude.

(C) As was indicated above, the transmitted power in the unstable region is very small. This is because the resonator no longer builds up energy from capturing photons over time and instead let's them loose on the cavity's surroundings. That is, the Q-factor of the resonator becomes very small as the resonator cannot confine the incoming photons any more.

References

[Saleh and Teich(2019)] B. Saleh and M. Teich, *Fundamentals of Photonics, 3rd Edition* (John Wiley & Sons, 2019).

[Milner(2023)] V. Milner, *PHYS 408 Cavity Lab Manual*, Tech. Rep. (University of British Columbia, 2023).